# CCR2 mediates hematopoietic stem and progenitor cell trafficking to sites of inflammation in mice

Yue Si,[1] Chia-Lin Tsou,[1] Kelsey Croft,[1] and Israel F. Charo[1,2]

[1]Gladstone Institute of Cardiovascular Disease, San Francisco, California. [2]Department of Medicine, University of California, San Francisco.

**HSCs are BM-derived, self-renewing multipotent cells that develop into circulating blood cells. They have been implicated in the repair of inflamed parenchymal tissue, but the signals that regulate their trafficking to sites of inflammation are unknown. As monocytes are recruited to sites of inflammation via chemoattractants that activate CCR2 on their surface, we investigated whether HSCs are also recruited to sites of inflammation through CCR2. Initial analysis indicated that in mice, CCR2 was expressed on subsets of HSCs and hematopoietic progenitor cells (HPCs) and that freshly isolated primitive hematopoietic cells ($Lin^-c\text{-}Kit^+$ cells) responded to CCR2 ligands in vitro. In vivo analysis indicated that after instillation of thioglycollate to cause aseptic inflammation and after administration of acetaminophen to induce liver damage, endogenous HSCs/HPCs were actively recruited to the peritoneum and liver, respectively, in WT but not *Ccr2*$^{-/-}$ mice. HSCs/HPCs recovered from the peritoneum successfully engrafted into the BM of irradiated primary and secondary recipients, confirming their self renewal and multipotency. Importantly, administration of exogenous WT, but not *Ccr2*$^{-/-}$, HSCs/HPCs accelerated resolution of acetaminophen-induced liver damage and triggered the expression of genes characteristic of the macrophage M2 or repair phenotype. These findings reveal what we believe to be a novel role for CCR2 in the homing of HSCs/HPCs to sites of inflammation and suggest new functions for chemokines in promoting tissue repair and regeneration.**

## Introduction

HSCs and hematopoietic progenitor cells (HPCs) proliferate within the BM and generate differentiated leukocytes that are released to the blood both constitutively and in response to infection or inflammation. HSCs provide a continuous source of hematopoietic cells through self renewal and proliferation, but small numbers of HSCs are present in the peripheral blood of naive animals (1, 2), and HPCs have been detected in peripheral tissues (3).

Although their functions in the periphery are unclear, HSCs and HPCs may have important roles in tissue repair and restoration of organ function (3, 4). For example, mobilization of endogenous HSCs or infusions of purified $CD34^+$ primitive hematopoietic cells improved left ventricular function after myocardial infarction (5–7), and in a phase I clinical trial, infusion of autologous $CD34^+$ cells improved liver function in patients with hepatic insufficiency (8). However, the molecular signals that control the trafficking of HSCs/HPCs to injured tissues are unknown.

Chemokines are secreted proteins that regulate the trafficking of leukocytes to sites of inflammation and injury. Among the most thoroughly characterized are monocyte chemoattractant proteins (MCPs). MCPs attract cells through activation of their cognate receptor, CCR2, which is expressed on monocytes (9). Mice genetically deficient in CCR2 exhibit markedly reduced tissue recruitment of monocytes to inflamed tissues in numerous disease models, including peritonitis (10), autoimmune encephalitis (11), tuberculosis (12), and atherosclerosis (13). Similar impairments in monocyte migration have been reported in mice lacking MCP-1 (CCL2) and MCP-3 (CCL7), which are the 2 major ligands for CCR2 (14–16).

We and others reported that CCR2 mediates the migration of mature monocytes not only from the BM into the blood (17, 18), but also from blood to tissues in response to inflammation (18). These results raised the possibility that CCR2 plays a crucial role in mediating the recruitment of HSCs and progenitor cells to inflamed tissues. In the present study, we report that CCR2 is expressed on primitive multipotent hematopoietic stem and progenitor cells and mediates recruitment of these HSCs/HPCs to sites of inflammation. Further, recruited HSCs/HPCs accelerated liver repair after drug-induced injury by differentiating into alternatively activated macrophages. These data support a critical role for CCR2 in HSC/HPC trafficking and suggest a mechanism by which BM-derived stem cells are recruited to participate in the repair and regeneration of damaged tissues.

## Results

*Expression of CCR2 on HSCs and myeloid progenitor cells.* To determine whether BM HSCs or HPCs express CCR2, we analyzed freshly isolated BM cells by multicolor FACS for 6 markers of stem cell/progenitor development and 6 markers of fully differentiated cells. Gating and flow analysis were carried out as described (19, 20). In naive mice, the fraction of cells expressing CCR2 increased as HSCs differentiated along the myeloid lineage (Figure 1). Interestingly, approximately 4% of BM long-term HSCs (LT-HSCs), defined as $Lin^-Sca1^+c\text{-}Kit^+IL7R\alpha^-Thy1.1^{lo}CD34^-$, and short-term HSCs (ST-HSCs), defined as $Lin^-Sca1^+c\text{-}Kit^+IL7R\alpha^-Thy1.1^{lo}CD34^+$ (19), expressed CCR2. Higher expression of CCR2 was detected in multipotent progenitors (MPPs), defined as $Lin^-Sca1^+c\text{-}Kit^+IL7R\alpha^-Thy1.1^-CD34^+$, as compared with the HSCs. A significant proportion (up to 30%) of common myeloid progenitors (CMPs) ($Lin^-Sca1^-c\text{-}Kit^+IL7R\alpha^-Thy1.1^-CD34^+CD16/32^{lo}$) and granulocyte-macrophage progenitors (GMPs) ($Lin^-Sca1^-c\text{-}Kit^+$

**Conflict of interest:** The authors have declared that no conflict of interest exists.

**Citation for this article:** *J Clin Invest.* 2010;120(4):1192–1203. doi:10.1172/JCI40310.

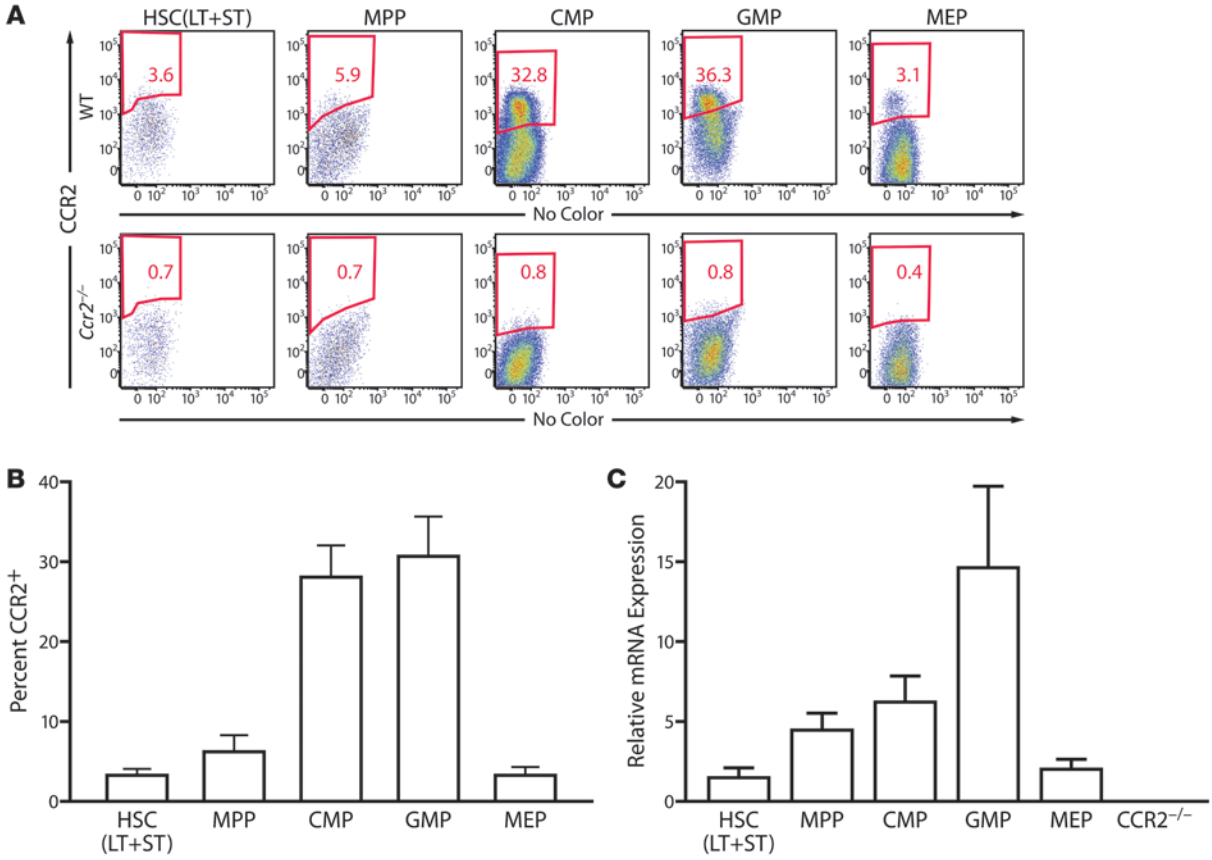


**Figure 1**

Expression of functional CCR2 on HSCs and HPCs. (**A**) BM HSCs and HPCs were identified by FACS, and the surface expression of CCR2 was quantified. LT-HSCs, defined as Lin$^-$Sca1$^+$c-Kit$^+$IL7Rα$^-$Thy1$^{lo}$CD34$^-$ cells. ST-HSCs, defined as Lin$^-$Sca1$^+$c-Kit$^+$IL7Rα$^-$Thy1$^{lo}$CD34$^+$ cells. MPPs, defined as Lin$^-$Sca1$^+$c-Kit$^+$IL7Rα$^-$Thy1$^-$CD34$^+$ cells. CMPs, common myeloid progenitors, defined as Lin$^-$Sca1$^-$c-Kit$^+$Thy1$^-$IL7Rα$^-$CD34$^+$CD16/32$^{lo}$ cells. GMPs, defined as Lin$^-$Sca1$^-$c-Kit$^+$ Thy1$^-$IL7Rα$^-$CD34$^+$CD16/32$^+$ cells. MEPs, megakaryocyte-erythroid progenitors, defined as Lin$^-$Sca1$^-$c-Kit$^+$Thy1$^-$IL7Rα$^-$CD34$^-$CD16/32$^-$ cells. The percentage of CCR2$^+$ cells in each group is indicated and is shown graphically in **B**. Values are mean ± SD. $n$ = 4 mice per genotype. Similar results were obtained in 5 independent studies. (**C**) qRT-PCR of *CCR2* mRNA in HSCs/HPCs. Total RNA was extracted from HSCs and the indicated HPCs. *CCR2* mRNA levels were determined by qRT-PCR and are expressed relative to the level in HSCs (arbitrarily set to 1.0). Values are mean ± SD.

IL7Rα$^-$Thy1.1$^-$CD34$^+$ CD16/32$^+$) were also CCR2 positive. Non-myeloid cells expressed little or no CCR2. Cell-surface expression of CCR2 in primitive hematopoietic stem cells correlated well with CCR2 mRNA levels, determined by quantitative real-time PCR (qRT-PCR) (Figure 1, B and C).

To determine whether CCR2 is required for HSCs to differentiate into myeloid lineage cells, we tested BM from WT and *Ccr2*$^{-/-}$ mice for the ability to form clonogenic myeloid progenitors in semisolid medium. Similar numbers of CFUs were recovered from WT and *Ccr2*$^{-/-}$ marrow (data not shown). Similarly, the addition of exogenous MCP-1 did not increase the size or number of colonies from WT marrow (data not shown). These data suggest that CCR2 is not required for the differentiation of HSCs to committed myeloid cells and are in agreement with earlier studies reporting normal production and differentiation of HSCs/HPCs in *Ccr2*$^{-/-}$ mice (21).

To assess CCR2-dependent functional responses, we sorted c-Kit$^+$Lin$^-$ primitive BM cells by FACS and analyzed their ability to migrate toward CCR2 ligands in a Boyden chamber chemotaxis assay. Phenotypic analysis of the input cells (Figure 2A) revealed that most (about 80%) were CD34$^+$. Analysis of the cells that responded to CCR2 ligand JE (Figure 2B) revealed a significant enrichment in CD34$^-$Sca1$^+$c-Kit$^+$Lin$^-$ (CD34$^-$SKL) cells, a population that is highly enriched in long-term repopulating HSCs (22, 23). Similar results were obtained with CCR2 ligand MCP-3 (Figure 2C).

CMPs and GMPs were purified and examined directly for chemotactic responses to JE, MCP-3, and stromal cell–derived factor 1 (SDF-1). Both CMPs and GMPs had specific chemotactic responses to JE and MCP-3 (Figure 2D). These cells also migrated in response to SDF-1, used as a positive control, as they are known to express its cognate receptor, CXCR4 (24, 25). To determine whether cells in the lower wells were clonogenic, we analyzed their ability to form colonies in semisolid methylcellulose. Quantification of CFUs (Figure 2E) in the lower wells confirmed that cells that had migrated in a CCR2-dependent manner were clonogenic. These data provide strong evidence that primitive hematopoietic cells undergo directional migration in response to CCR2 ligands.

*CCR2 mediates active recruitment of endogenous HSCs/HPCs to sites of inflammation*. To determine whether CCR2 mediates in vivo trafficking of HSCs/HPCs to sites of inflammation, we utilized the thioglycollate model of aseptic peritonitis. Previously, we

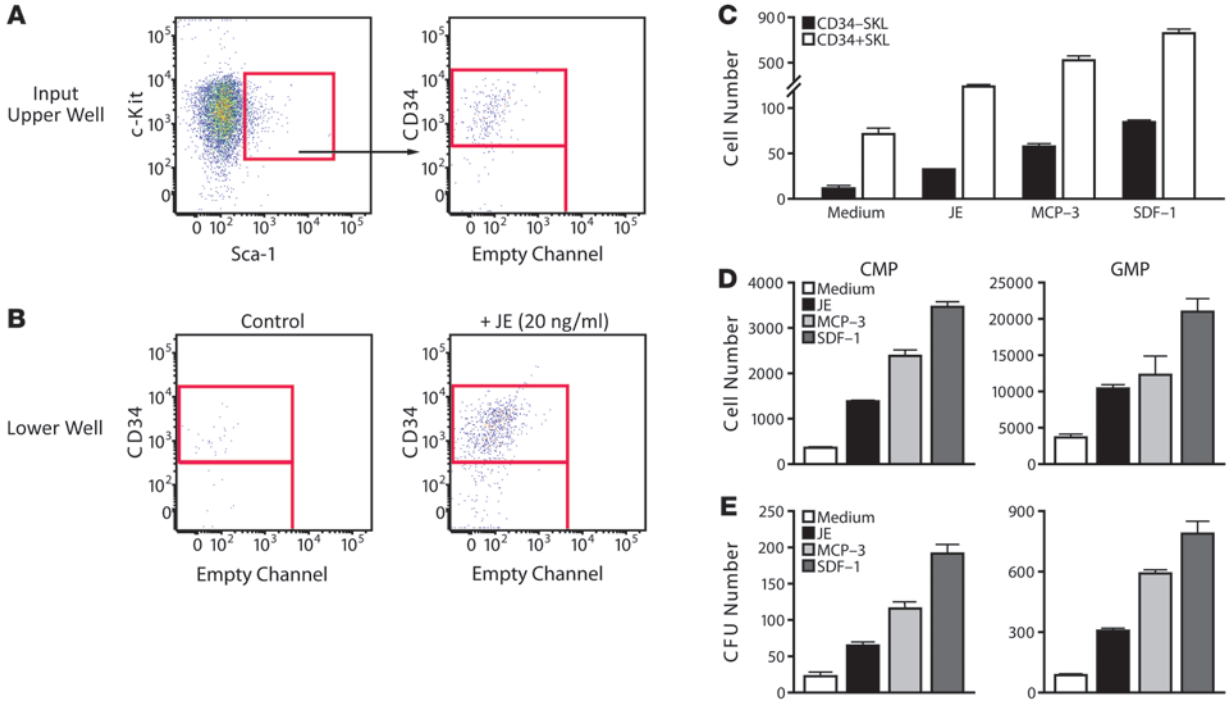


**Figure 2**
Chemotaxis of HSCs/HPCs to CCR2 ligands. c-Kit$^+$Lin$^-$ BM cells were placed into the upper chamber of a Boyden chemotaxis chamber. MCP-1 or MCP-3 was added at the indicated concentrations to the lower chambers, and cells that migrated into the lower chambers were quantified by FACS. (**A**) Phenotypic analysis of input c-Kit$^+$Lin$^-$ cells for c-Kit, Sca-1, and CD34. (**B**) Analysis of cells that migrated to the lower chamber in response to JE (mMCP-1) or buffer control. (**C**) Quantification of primitive CD34$^-$Sca1$^+$c-Kit$^+$Lin$^-$ (CD34 – SKL) cells that migrated to the lower well in response to the CCR2 ligands JE and MCP-3 or the CXCR4 ligand SDF-1. (**D**) Chemotaxis of CMPs and GMPs to JE, MCP-3, and SDF-1. (**E**) Quantification of clonogenic cells that underwent chemotaxis in response to JE, MCP-3, and SDF-1. Values are mean ± SD.

showed that thioglycollate increases the production of MCP-1 and MCP-3 and induces rapid trafficking of monocyte/macrophages into the peritoneum (18). It was not known, however, whether this trafficking included HSCs/HPCs.

In naive mice, few HSCs/HPCs were present in the peritoneum, as determined by the ability to form colonies (Figure 3A). In contrast, thioglycollate induced robust trafficking of HSCs/HPCs to the peritoneum in WT but not *Ccr2*$^{-/-}$ mice. The typical morphology of the CFUs recovered from the peritoneum of WT mice is shown in Figure 2B. Multiparameter FACS analysis revealed significantly fewer peritoneal Lin$^-$ cells in *Ccr2*$^{-/-}$ mice (Figure 3C), reflecting decreases in both Lin$^-$Sca1$^+$c-Kit$^+$ (SKL, an enriched population of HSCs) and Lin$^-$Sca1$^-$c-Kit$^+$ myeloid progenitors (MPs) (Figure 3, C and D). *Ccr2*$^{-/-}$ mice also had more Lin$^-$ cells in blood (Figure 3E). These data are consistent with a role for CCR2 in mediating the trafficking of clonogenic HSCs/HPCs to the peritoneum in response to thioglycollate.

To establish the relative contributions of individual MCP ligands to CCR2 activation and HSC/HPC recruitment to sites of inflammation, we used mice genetically deficient in MCP-1, MCP-3, or MCP-2 and MCP-5. After thioglycollate challenge, the percentage of Lin$^-$Sca1$^+$c-Kit$^+$and Lin$^-$Sca1-c-Kit$^+$ MPs in cells recovered from the peritoneum was significantly decreased in *Mcp1*$^{-/-}$ and *Mcp3*$^{-/-}$ mice, but not in *Mcp2*$^{-/-}$*Mcp5*$^{-/-}$ mice (Figure 3F).

*CCR2-recruited HSCs/HPCs proliferate and differentiate at site of inflammation*. Next, we asked whether CCR2-recruited HSCs/HPCs proliferate and differentiate at sites of inflammation. WT mice were treated with thioglycollate, and Lin$^-$ cells were obtained from the peritoneum, labeled with CFSE, and injected into the peritoneum of thioglycollate-challenged *Ccr2*$^{-/-}$ mice (Figure 4A). After 48 hours, quantification of CFSE intensity revealed multiple, distinct peaks (Figure 4B) whose intensity decreased by 50% from peak to peak (Figure 4C), confirming that the injected HSCs/HPCs originally isolated from inflamed peritoneum proliferated. Analysis of the donor CD45.1$^+$ cells for markers of myeloid and lymphoid lineage differentiation showed that Lin$^-$ cells recruited to peritoneum differentiated into both myeloid and lymphoid cells, as shown by expression of CD11b, CD11c, Gr1, CD3, and B220 (Figure 4D).

*HSCs/HPCs recruited to the inflamed peritoneum reconstitute myeloid and lymphoid lineages in lethally irradiated mice*. We next sought to determine whether the cells recovered from the peritoneum in response to thioglycollate were capable of in vivo self renewal and long-term repopulation of the BM. In a competitive repopulation assay, Lin$^-$ cells from the peritoneum of thioglycollate-treated CD45.2 WT mice were injected into the blood of irradiated CD45.1 WT recipients (Figure 5A). In the recipients, approximately 16% of the peripheral blood leukocytes at 8 weeks and approximately 10% at 16 weeks were derived from the CD45.2 mice (Figure 5B). To determine whether the peritoneum-derived cells contained true, long-term self-replicating stem cells, BM from the primary recipients was transplanted into lethally irradiated secondary (CD45.1) recipients. At 16 weeks following transplant, approximately 3% of the cells were CD45.2$^+$, confirming the presence of long-term HSCs in the donor population. Analysis of CD45.2$^+$ peripheral blood cells from the primary recipients revealed

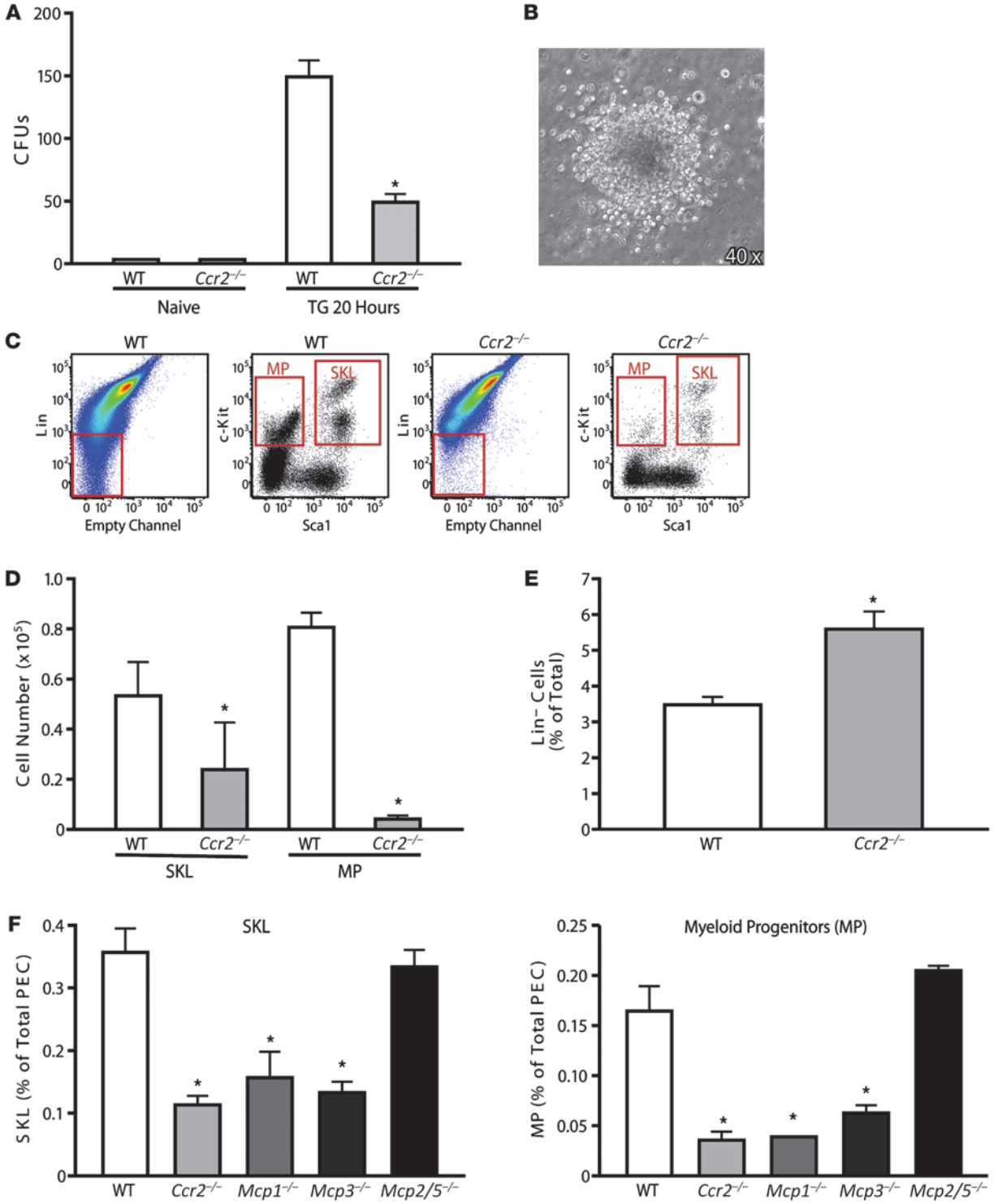


**Figure 3**

CCR2 mediates the recruitment of HSCs/HPCs to the peritoneum. (**A**) Thioglycollate (TG) was injected into the peritoneum of WT and *Ccr2*$^{-/-}$ mice, and HSCs/HPCs recruited after 20 hours were quantified as CFUs. Values are mean ± SD. *$P < 0.01$ versus WT. $n = 8$ per genotype. (**B**) Micrograph of typical CFU-GM recovered from the peritoneum of WT mice. (**C**) Representative FACS plots of peritoneal leukocytes from WT and *Ccr2*$^{-/-}$ mice. MPs were defined as Lin$^-$Sca1$^-$c-Kit$^+$, and enriched HSC populations (SKL) were defined by the markers of Lin$^-$Sca1$^+$c-Kit$^+$. (**D**) Quantification of the FACS data. Values are mean ± SD. $n = 8$ per genotype. *$P < 0.05$. (**E**) Quantification of Lin$^-$ cells in blood in WT and *Ccr2*$^{-/-}$ mice after thioglycollate injection. Values are mean ± SD. $n = 8$ mice per genotype. *$P < 0.05$. (**F**) The number of SKLs (Lin$^-$Sca1$^+$c-Kit$^+$) and MPs (Lin$^-$Sca1$^-$c-Kit$^+$) recruited to the peritoneum 20 hours after injection of thioglycollate was quantified by FACS. Values are mean ± SD. *$P < 0.01$ versus WT. WT, $n = 5$; *Mcp1*$^{-/-}$, $n = 5$; *Mcp3*$^{-/-}$, $n = 5$; *Mcp2*$^{-/-}$*Mcp5*$^{-/-}$, $n = 5$.

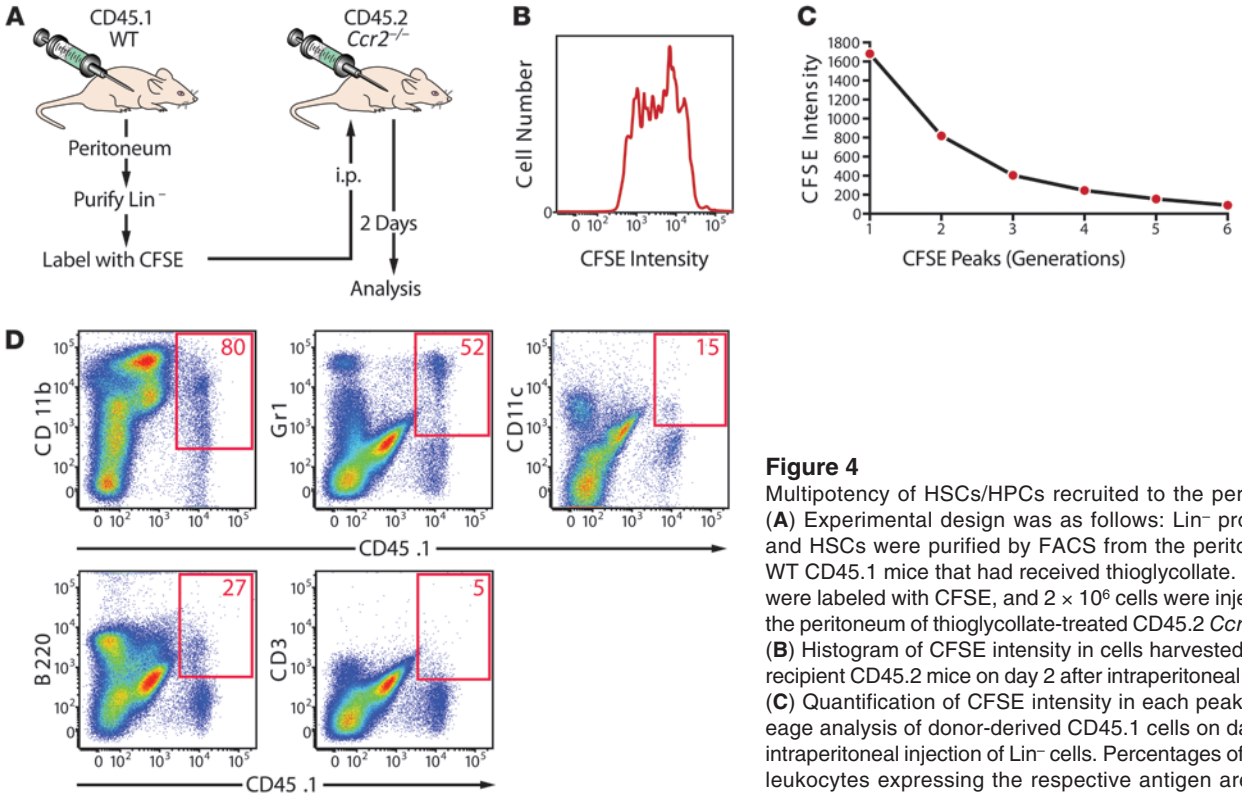


**Figure 4**
Multipotency of HSCs/HPCs recruited to the peritoneum. (**A**) Experimental design was as follows: Lin$^-$ progenitors and HSCs were purified by FACS from the peritoneum of WT CD45.1 mice that had received thioglycollate. The cells were labeled with CFSE, and $2 \times 10^6$ cells were injected into the peritoneum of thioglycollate-treated CD45.2 *Ccr2*$^{-/-}$ mice. (**B**) Histogram of CFSE intensity in cells harvested from the recipient CD45.2 mice on day 2 after intraperitoneal injection. (**C**) Quantification of CFSE intensity in each peak. (**D**) Lineage analysis of donor-derived CD45.1 cells on day 2 after intraperitoneal injection of Lin$^-$ cells. Percentages of CD45.1$^+$ leukocytes expressing the respective antigen are shown. Representative data from 3 independent experiments.

fully differentiated B cells, T cells, granulocytes, and monocytes (Figure 5C). In similar studies with *Ccr2*$^{-/-}$ mice as donors, extremely few CD45.2 cells were detected in the blood 16 weeks after primary transplantation (data not shown). These results indicate that after thioglycollate-induced peritonitis, multipotent, long-term self-replicating HSCs are actively recruited to the site of inflammation and their recruitment is highly dependent on CCR2.

*CCR2-dependent homing of endogenous HSCs/HPCs to the liver after acetaminophen-induced injury*. To determine whether endogenous HSCs/HPCs home to tissue in response to injury or disease, we induced hepatotoxicity by intraperitoneal administration of acetaminophen (APAP) (300 mg/kg). This dose produced transient elevations of liver transaminase enzymes and mild histological damage in WT mice but more severe parenchymal damage in *Ccr2*$^{-/-}$ mice (Figure 6A). In naive mice, FACS analysis 48 hours after challenge with PBS showed similar numbers of CD45$^+$Lin$^-$c-Kit$^+$ hematopoietic stem and progenitors in the liver in WT and *Ccr2*$^{-/-}$ mice (Figure 6B). After administration of APAP, however, significantly more CD45$^+$Lin$^-$c-Kit$^+$ cells were recruited to the liver in WT mice (Figure 6B). Conversely, there were relatively more colony-forming HSCs/HPCs in the blood in *Ccr2*$^{-/-}$ mice (Figure 6C).

We next asked whether these CD45$^+$Lin-c-Kit$^+$ cells in liver include self-renewing hematopoietic stem cells. Cells from the livers of naive, and APAP-treated CD45.2 mice were analyzed by FACS, using a combination of markers and light scatter to identify lineage-negative cells, which were then transfused into irradiated CD45.1 mice. Four months later, CD45.2 cells had populated the monocyte/macrophage (CD11b$^+$) compartment of the blood in the recipient mice, the granulocyte compartment (Gr1$^+$), the B cell compartment (B220$^+$), and the T cell compartment (CD3$^+$), demonstrating the multipotency of the cells harvested from the liver (Figure 6D).

*Attenuation of APAP-induced liver injury by WT but not CCR2*$^{-/-}$ *HSCs/HPCs*. Finally, we determined whether recruitment of HSCs/HPCs to the liver altered the response to APAP-induced injury. CD45.2$^+$ WT or *Ccr2*$^{-/-}$ Lin$^-$ BM cells were sorted by FACS and injected intravenously into CD45.1$^+$ WT mice that had received APAP. As expected, APAP induced dramatic increases in serum aspartate aminotransferase (AST) and alanine aminotransferase (ALT) levels. Significantly, infusion of WT, but not *Ccr2*$^{-/-}$, Lin$^-$ BM cells decreased serum AST (Figure 7A) and ALT levels (Figure 7B), indicating that recruitment of HSCs/HPCs to the liver is protective. To investigate the mechanism, we quantified the recruitment of the CD45.2$^+$ donor cells to liver by FACS analysis. Significantly more WT than *Ccr2*$^{-/-}$ cells homed to the APAP-injured liver (Figure 8, A–C). Analysis of these cells revealed that they had differentiated primarily into CD11b$^{hi}$F4/80$^{lo}$ macrophages (Figure 8, D–G). qRT-PCR analysis of mRNA extracted from purified infiltrating macrophages (IMs) and Kupffer cells (KCs) revealed high levels of CCR2 only in IMs (Figure 8H). The IMs, which were derived from the transferred Lin$^-$ HSCs/HPCs, expressed genes characteristic of alternatively activated (M2) macrophages, including Ym1, Fizz-1, and Mrc (Figure 8, I and J).

## Discussion

CCR2 mediates the directed migration of mature monocyte/macrophages to areas of inflammation and injury (26, 27). Here we report that CCR2 is expressed on a subset of self-renewing LT-HSCs and ST-HSCs as well as on MPs. CCR2 mediated the

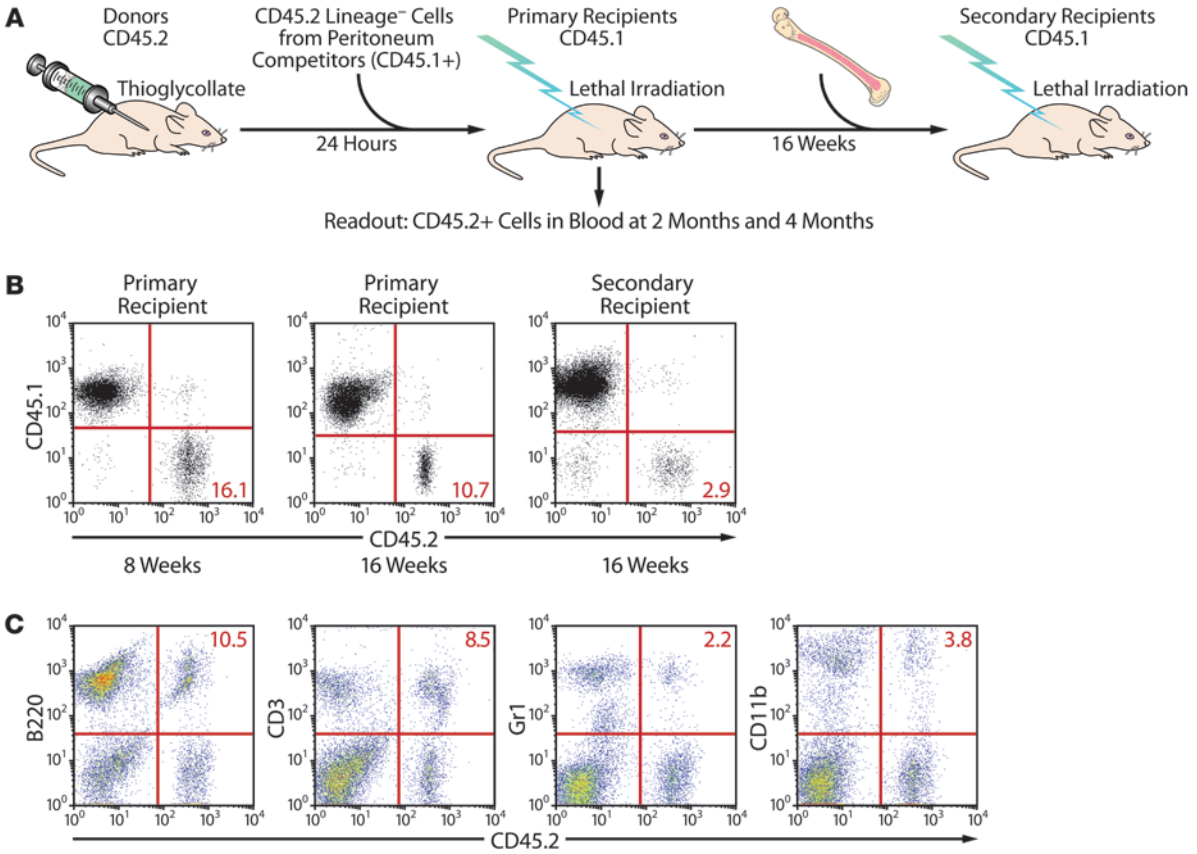


**Figure 5**

BM engraftment and long-term reconstitution of myeloid and lymphoid lineages with peritoneum-derived HSCs. (**A**) Peritoneal Lin⁻ leukocytes from 12 thioglycollate-injected WT CD45.2 mice or *Ccr2*$^{-/-}$ mice were collected, mixed with 1 × $10^5$ WT CD45.1 BM cells, and injected intravenously into lethally irradiated WT CD45.1 primary recipients. After 16 weeks, BM from the primary recipients was injected into lethally irradiated CD45.2 WT secondary recipients. (**B**) FACS plots show the percentage of CD45.2⁺ cells in the peripheral blood of the primary recipients at 8 and 16 weeks after transplantation and a secondary recipient at 16 weeks after transplantation. No engraftment was identified in mice injected with *Ccr2*$^{-/-}$Lin⁻ peritoneal cells (data not shown). At 16 weeks, the mean percentage (±SD) of donor chimerism from primary and secondary recipients was 9 ± 3.6 and 2 ± 0.9. Shown are representative FACS plots. (**C**) Lineage analysis of donor CD45.2 cells in the blood of primary recipients 16 weeks after transplantation. Numbers in the upper right quadrant are percentages of CD45.2⁺ peripheral blood cells expressing the respective markers. Shown are representative FACS plots.

chemotaxis of Lin⁻ HSCs/HPCs in vitro and the accumulation of primitive, self-renewing stem cells to sites of tissue inflammation in vivo. Specifically, recruitment of HSCs/HPCs to the peritoneum after instillation of thioglycollate and to the liver in response to APAP was strongly CCR2 dependent. Recruited HSCs/HPCs contributed to tissue repair, as evidenced by the normalization of circulating liver enzymes. Improved liver function coincided with polarization of hepatic macrophages, derived from adoptively transferred HSCs/HPCs, to the M2 phenotype. These results demonstrate a role for CCR2 in the recruitment of hematopoietic stem and progenitor cells to sites of injury, where they may contribute to tissue repair by in situ hematopoiesis and differentiation.

Although HSCs/HPCs are present in low numbers in the blood, their functional significance outside of the BM has been unclear (2). HSCs/HPCs recirculate between the BM and the lymph and differentiate into dendritic cells after entering peripheral tissues (3). HSCs/HPCs express TLR2 and TLR4, and ligation of these receptors with LPS drives their differentiation into mature, lineage-positive cells (28). These findings suggested a means of rapid replenishment of the innate immune cells but did not identify the signals critical for their recruitment and trafficking. Our findings suggest that the signals that recruit fully differentiated monocytes to sites of inflammation are also critical for recruitment of circulating HSCs/HPCs to the peripheral tissues, evidently to contribute to the resolution of the inflammation and injury.

In preliminary studies, we noted CCR2 on the surface of primitive hematopoietic cells. Further analysis revealed a progressive increase in the fraction of cells expressing CCR2 as differentiation proceeded from self-renewing HSCs, to MPPs, to cells committed to the myeloid lineages (CMPs and GMPs), and finally to fully differentiated monocytes. Similar trends were seen when CCR2 mRNA was quantified. This is consistent with the finding of CCR2 mRNA transcripts in a subset of primitive hematopoietic cells, though CCR2 was not shown to be present on the cell surface (29). Whether or not CCR2 transcription is controlled by differentiation per se is unknown.

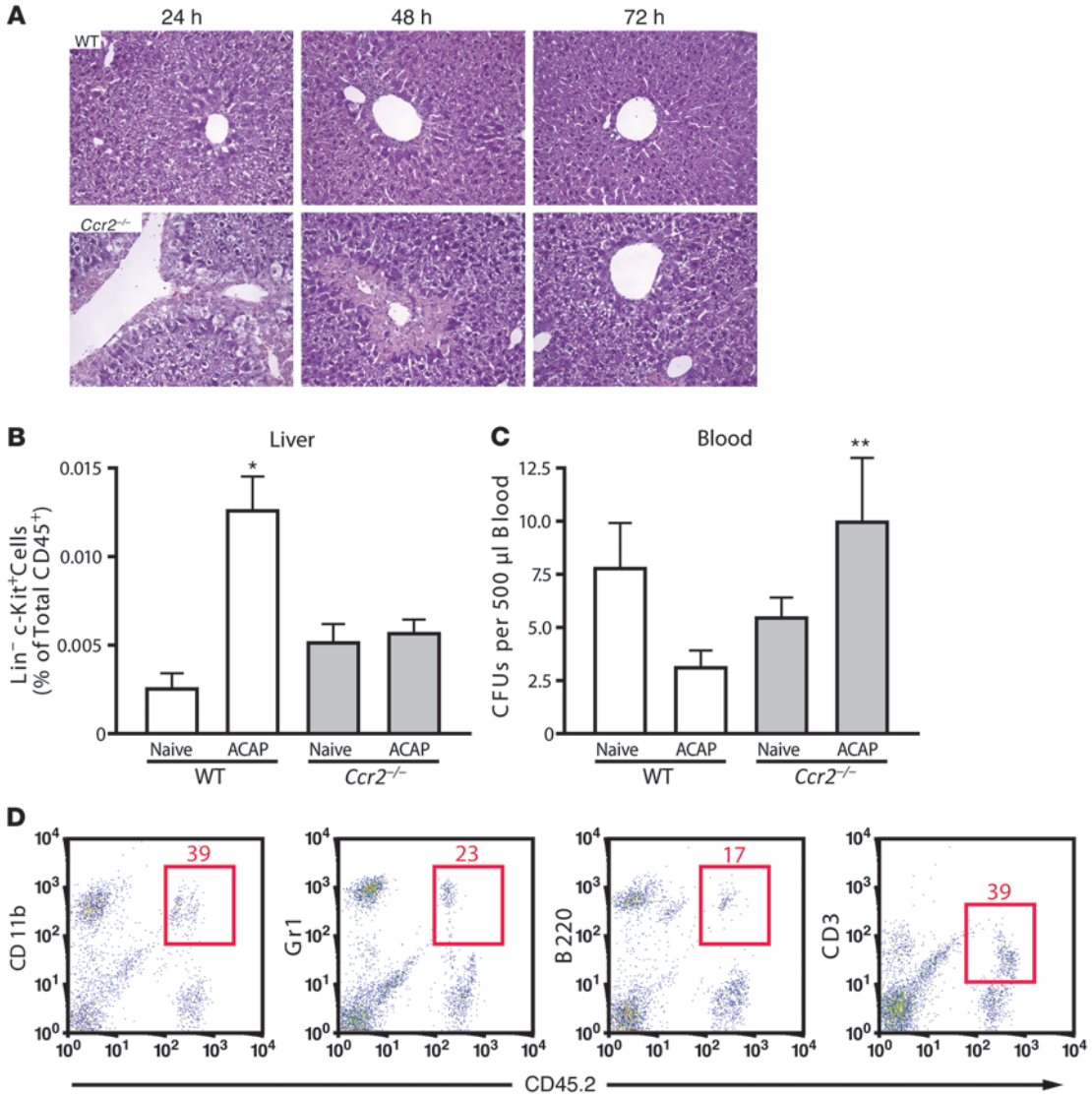


**Figure 6**

Protective role of CCR2-dependent recruitment of HSCs/HPCs to the liver. WT or *Ccr2*$^{-/-}$ mice were injected intraperitoneally with APAP (300 mg/kg) and analyzed 48 hours later. (**A**) Histopathology of the liver from WT and *Ccr2*$^{-/-}$ mice. At 24 and 48 hours after APAP challenge, liver sections from WT mice exhibited minor centrilobular injury with increased infiltration of inflammatory cells at 48 hours; sections from *Ccr2*$^{-/-}$ mice had greater necrotic injury. At 72 hours, the WT mice had greater resolution of injury than *Ccr2*$^{-/-}$ mice. Original magnification, ×400. (**B**) Quantification of CD45$^{+}$Lin$^{-}$c-Kit$^{+}$ cells in the liver. Values are mean ± SD of the percentage of total nonhepatocytes in the liver. Data shown are representative of 3 independent experiments; $n = 4$ mice per genotype. *$P < 0.01$ versus naive WT. (**C**) Clonogenic assays to quantify CFUs in the blood of WT and *Ccr2*$^{-/-}$ mice before and 48 hours after APAP treatment. Values are mean ± SD. $n = 4$ mice per genotype. **$P < 0.05$ versus naive WT mice. (**D**) Cells isolated from the livers of APAP-treated mice are multipotent. CD45.2 mice were treated with APAP, and Lin$^{-}$ cells were isolated from their livers and infused into CD45.1 recipients. Analysis of the blood of the recipient mice for CD45.2$^{+}$ T cells (CD3), B cells (B220), granulocytes (Gr-1), and monocytes (CD11b). The percentage of CD45.2$^{+}$ cells expressing each marker is shown.

To determine whether CCR2 on HSCs or HPCs is functional, we combined in vitro and in vivo approaches. Chemotaxis is the hallmark function of the chemokine family, and using standard in vitro assays, we found that both CCR2-expressing HSCs and progenitors exhibited directional migration in response to CCR2 ligands. A more stringent test of chemotaxis is the ability to home to sites of inflammation in vivo. The model of thioglycollate-induced peritonitis is widely used for this purpose, and we and others have found that CCR2 drives the peritoneal recruitment of approximately 75% of the fully differentiated monocyte/macrophages in this model (10, 30). Surprisingly, we also found that significant numbers of HSCs and HPCs were recruited to the peritoneum in a CCR2-dependent manner. These recruited cells included long-term self-renewing stem cells, as demonstrated by their ability to repopulate multiple hematopoietic lineages in secondary transplant recipients. These data provide strong evidence that CCR2 mediates homing of HSCs and HPCs to sites of inflammation.

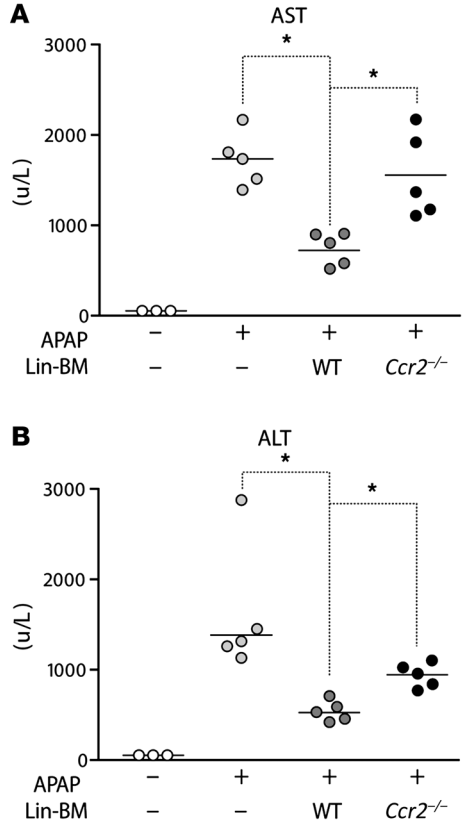


**Figure 7**

Adoptive transfer of CCR2$^+$Lin$^-$ BM cells reduces APAP liver injury. CD45.1 mice were treated with APAP. Four hours later, they received adoptive transfers of CD45.2 Lin$^-$ BM cells from WT or *Ccr2*$^{-/-}$ mice. Serum was collected 44 hours later and analyzed for markers of liver damage. (**A**) AST. (**B**) ALT. Symbols represent individual mice. Bars represent the means. *$P < 0.05$ versus mice that received WT Lin$^-$ BM cells.

Chemokine receptors regulate the trafficking of cells into and out of the BM. CXCR4 is expressed on HSCs and HPCs, and antagonists of this receptor have been used in human clinical trials to facilitate release of stem cells from the BM (31, 32). We and others have found that CCR2 mediates the release of mature monocytes from the BM (18, 33). *Ccr2*$^{-/-}$ mice have decreased numbers of "inflammatory" (Ly6C$^{hi}$) monocytes in the blood and fail to increase the number of these monocytes in response to inflammation or infection (17, 18). Results from the current study suggest that although HSCs/HPCs use CCR2 to home to sites of inflammation, they appear to be less dependent upon CCR2 than monocytes for egress from the BM. Thus, after APAP-induced liver injury, we find similar or increased numbers of HSCs/HPCs in the blood in *Ccr2*$^{-/-}$ and WT mice, but their numbers are significantly decreased in the liver in *Ccr2*$^{-/-}$ mice.

Previously, we reported that *Ccr2*$^{-/-}$ mice have exaggerated liver necrosis after APAP ingestion, implying a protective or reparative role for recruited macrophages (34). Consistent with this finding, Holt et al. found that a population of macrophages resembling M2 macrophages was present in the liver of WT, but not *Ccr2*$^{-/-}$ mice, after APAP injection (35). In the current study, exogenously administered WT, but not *Ccr2*$^{-/-}$, HSCs/HPCs, differentiated into M2 macrophages in the livers of APAP-treated mice. Giving the rarity of transdifferentiation and cell fusion, the robust local differentiation of HSCs/HPCs into M2 (reparative) macrophages might be an important component of the improvement in liver function observed after the administration of BM stem cells in human clinical studies (8, 36).

Because HSCs differentiate into mature monocytes, it was important to determine whether the endogenous or the infused exogenous BM Lin$^-$ cells were HSCs or HPCs when they were recruited to the inflamed peritoneum or injured liver or had already differentiated into monocytes. Several lines of evidence support the claim that they were HSCs/HPCs. First, multicolor FACS analysis confirmed that the CD45$^+$ donor cells recovered from the injured liver and from the peritoneum after thioglycollate treatment were Lin$^-$c-Kit$^+$. Second, cells recovered from inflammation sites formed hematopoietic colonies in semisolid methylcellulose medium. Third, cells recovered after thioglycollate treatment from the peritoneum of WT mice, but not *Ccr2*$^{-/-}$ mice, repopulated the BM of lethally irradiated recipient mice, a caveat being that fewer (~60%) Lin$^-$ cells were recovered from the peritoneum of *Ccr2*$^{-/-}$ mice, giving the WT cells a relative competitive advantage. Similar results were obtained with Lin$^-$ cells recovered from the livers of APAP-treated mice. These findings show that CCR2 mediates the homing of HSCs/HPCs to injured tissue and that these cells provide a disease-modifying benefit above and beyond that provided by the recruitment of mature CCR2$^+$ monocytes.

HSCs have been implicated in the recovery of organs from inflammatory insults, including myocardial repair after ischemic injury (4, 37–39) and hepatic function in patients with liver diseases (8, 36). Studies in mice and humans have documented a modest but reproducible improvement in left ventricular function after infusion of unfractionated or progenitor-enriched BM cells (5–7, 40). Although HSCs do not likely differentiate into authentic cardiomyocytes (41, 42), BM-derived cells that retain hematopoietic markers have been found in the heart and likely mediate improved myocyte function through paracrine effects (43). Similarly, intraperitoneal delivery of HSCs/HPCs reduces alcohol-induced liver damage and improves survival in immunodeficient mice (44), and infusion of G-CSF–primed hematopoietic stem cells accelerates regeneration and improves survival after liver injury or liver transplant (45, 46). Although the clinical improvements in these preclinical and clinical studies have generally been modest, increasing the homing efficiency of the HSCs/HPCs to the injured or ischemic tissue might well lead to more robust results. In 2 different models of inflammation and tissue injury, we found that CCR2 plays an important role in the recruitment of endogenous as well as exogenous HSCs/HPCs. It is worth noting, however, that less than 5% of the HSCs are CCR2$^+$. CCR2 may thus identify a population of HSCs that is particularly efficient at homing to injured tissues. Enriching for HSCs with high-level CCR2 expression or directly upregulating CCR2 may significantly enhance HSC homing to injured tissues and provide a path forward for optimizing future clinical trials.

In summary, we found that subsets of primitive HSCs and HPCs in BM express functional CCR2. In 2 different models of inflammation/injury, endogenous HSCs/HPCs were rapidly recruited from the BM to sites of tissue inflammation. HSCs/HPCs recovered from sites of injury remained multipotent and contributed to the reconstitution of lethally irradiated mice. Interestingly, HSCs/HPCs had a protective effect in APAP-induced liver injury, possibly by differentiation into alternatively activated macrophages. Circulating HSCs/HPCs might represent a "reserve" pool of cells competent to undergo proliferation and differentiation locally in

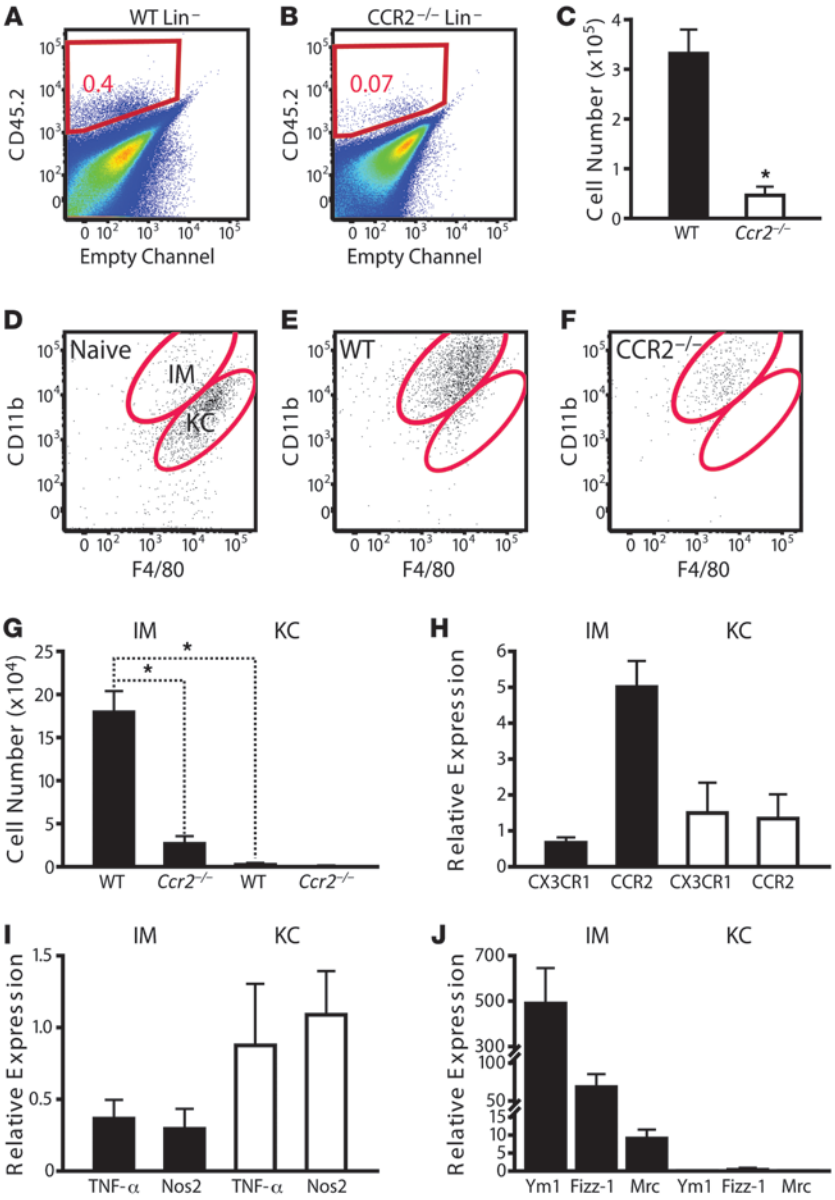


**Figure 8**

CCR2$^+$Lin$^-$ BM cells differentiate into M2 macrophages in APAP-injured liver. (**A**–**C**) Identification of donor-derived CD45.2 cells in APAP-treated liver. At 48 hours after transfer of CD45.2$^+$ WT or *Ccr2*$^{-/-}$ Lin$^-$ BM cells into APAP-treated CD45.1 mice, liver nonhepatocytes were isolated and stained for CD45.2 (**A** and **B**). Representative FACS plots are shown. (**C**) Number of donor-derived CD45.2$^+$ cells per 1 million of nonhepatocytes are shown. Values are mean ± SD. *$P$ < 0.01 vs. WT. (**D**–**G**) Donor Lin$^-$ BM cells differentiate primarily into IMs. (**D**) Two macrophage populations in the liver of mice 48 hours after APAP challenge. Nonhepatocytes were isolated and stained with anti-CD45.2, anti-CD11b, and anti-F4/80. CD45.2$^+$ cells were gated and evaluated for the expression of F4/80 and CD11b to separate IMs from KCs. (**E**) IMs and KCs from mice who received WT CD45.2$^+$Lin$^-$ cells. (**F**) IMs and KCs from mice who received *Ccr2*$^{-/-}$ CD45.2$^+$Lin$^-$ cells. (**G**) Quantification of FACS plots. Values are mean ± SD per 1 million nonhepatocytes. *$P$ < 0.05 versus IM cells derived from WT Lin$^-$ BM cells. (**H**–**J**) Hepatic IMs and KCs from mice 48 hours after APAP challenge were purified by FACS. RNA was extracted, and mRNA levels were determined by qRT-PCR, including (**H**) chemokine receptors CCR2 and CX3CR1 and genes associated with classical (M1) macrophage activation (**I**) or M2 macrophage activation (**J**). Values are mean ± SD.

tissues in response to pathogens. Such local hematopoiesis would represent another layer of host defense or, as illustrated for liver damage, organ repair. Understanding the temporal and spatial relationships governing the recruitment of these cells will provide a more rational framework for developing cell-based therapies.

## Methods

*Mice*. *Ccr2*$^{-/-}$, *Mcp1*$^{-/-}$, *Mcp3*$^{-/-}$, and *Mcp2*$^{-/-}$*Mcp5*$^{-/-}$ mice were generated as described (10, 18, 47) and backcrossed for 10 generations onto a C57BL/6 background. Congenic C57BL/6J (CD45.2$^+$) and B6.SJL-PtrcaPep3b/BoyJ (B6.BoyJ) mice (CD45.1$^+$) were purchased from Jackson Laboratory and maintained in our animal facility. *gfp*$^{+/-}$ (*CX3CR1*) mice were generated as described (48) and were provided by S. Jung (Weizmann Institute of Science, Rehovot, Israel) and D. Littman (New York University Medical Center, New York). *Mcp1*$^{-/-}$ mice (47) were provided by B.J. Rollins (Dana-Farber Cancer Institute, Boston, Massachusetts). All mice were backcrossed 10 times onto the C57BL/6 background. Mice were housed and bred with littermate controls in pathogen-free conditions and were studied at 6–12 weeks of age. All mouse experiments were approved by the University of California, San Francisco, Animal Care Committee.

*Isolation of BM cells*. BM cells were flushed from the tibia and femur with Iscove's modified Dulbecco's medium (Gibco-BRL; Invitrogen) containing 2% FCS (Hyclone Laboratories). Cells were filtered through a nylon screen (70 mm) to obtain single-cell suspensions. Red blood cells were depleted with ACK lysis buffer (150 mM $NH_4Cl$, 1 mM $KHCO_3$, 0.1 mM EDTA).

*Isolation of cells from the liver*. Nonhepatocytes were isolated from WT and *Ccr2*$^{-/-}$ mice by collagenase digestion and differential centrifugation as described (49) with slight modifications. Briefly, the liver was perfused in situ with liver perfusion medium (Invitrogen), followed by digestion medium (Invitrogen) for 3 minutes. After digestion, the liver was excised and minced, and the suspension was filtered through mesh (70 mm). The filtrate was centrifuged twice at 50 *g* at 4°C for 5 minutes. The supernatant was collected and centrifuged at 1,000 *g* for 10 minutes, and the pellet was resuspended in PBS with 0.1% BSA and 2 mM EDTA.

*Hematopoietic progenitor assays*. Recombinant GM-CSF, IL-3, and stem cell factor were obtained from Peprotech. Recombinant erythropoietin was from Amgen. Briefly, low-density mononuclear BM cells were isolated from the BM with Ficoll Hystopaque-1119 (Sigma-Aldrich), washed in PBS/0.1% BSA, and resuspended in Iscove's modified Dulbecco's medium with 10% fetal bovine serum. For cells from blood or peritoneum, cells were lysed with ACK buffer and washed once with PBS before plating. Cells were cultured in triplicate on 35-mm plates (BD) at a final concentration of $2 \times 10^4$ low-density mononuclear cells or leukocytes from 500 μl of peripheral blood in 40% methylcellulose (Stem Cell Technologies), 30% FCS, 1% Iscove's modified Dulbecco's medium, 200 U/ml penicillin and streptomycin, 80 mM 2-mercaptoethanol (Sigma-Aldrich), 50 ng/ml murine stem cell factor, 10 ng/ml murine GM-CSF, 2 U/ml recombinant erythropoietin, and 100 U/ml IL-3. To evaluate CFUs in the peritoneum, total peritoneal nucleated cells from 1 mouse were plated in triplicates. CFUs were scored 7–14 days after the initiation of the culture in 5% $CO_2$ at 37°C.

*Antibodies and flow cytometry*. BM cells were harvested from long bones as described above, and red blood cells were depleted using ACK lysis buffer (150 mM $NH_4Cl$, 1 mM $KHCO_3$, 0.1 mM EDTA). $Lin^-c\text{-}Kit^+Sca1^+CD34^-Thy1.1^{lo}IL7R\alpha^-$ HSCs were stained as described (19). CD16/32 was further used in combination with the markers cited above to define subsets of progenitors, as described (19, 20). Lineage markers included Gr1, Mac1, B220, CD3, MHC-II, and NK1.1. The following antibodies used for FACS analysis were purchased from BioLegend: anti-Sca-1 (clone D7), k isotype control (clone RTK2758), and Thy1 (clone 30-H12). Anti-CD34 (clone RAM34) was from eBioscience. The following antibodies for flow cytometry were purchased from BD Biosciences — Pharmingen: anti–MHC II (clone AF6-120.1), anti-NK1.1 (clone PK136), anti-Gr1 (clone RB6-8C5), anti-Mac1 (clone), anti-B220 (clone RA3-6B2), anti-CD3 (clone 145-2C11), anti–IL-7Rα (clone SB/119), anti-CD117 (clone 2B8), k isotype control (clone A95-1), anti CD16/CD32 (clone 2.4G2), anti-CD45.2 (clone 104), anti-CD45.1 (clone A20), anti-CD11c (clone HL3), anti-CD19 (clone 1D3), and streptavidin-APC and streptavidin-PE. The antibody against F4/80 was from Caltag Laboratories. The antibody against murine CCR2 has been described (50).

Nucleated cells from BM, blood, peritoneum, or liver were washed with staining buffer (PBS with 0.1% BSA and 2 mM EDTA), and $3 \times 10^6$ cells/ml were stained with mouse anti-mouse CD16/CD32 (1:50; Caltag Laboratories) for 30 minutes to block Fc receptors. After washing to remove excess antibody, the cells were incubated simultaneously with the antibodies of interest for 30 minutes at 4°C. Cells were washed twice with staining buffer and analyzed by flow cytometry. The antibody against murine CCR2 was kindly provided by M. Mack (University of Munich, Germany) and has been described (50). When stained with CCR2 antibody, a 3-step staining procedure was used as described (18, 50).

Flow cytometry analyses were conducted on a FACS LSRII or FACSCalibur (BD). FACS sorting was carried out on a FACSVantage or FACSAriaII (BD), and the data were analyzed with FlowJo software (Treestar).

*Thioglycollate-induced peritonitis*. Peritonitis was induced by instillation of thioglycollate into WT, *Ccr2*$^{-/-}$, *Mcp3*$^{-/-}$, *Mcp1*$^{-/-}$, and *MCP2*$^{-/-}$*MCP5*$^{-/-}$ mice as described (10, 18). Peritoneal leukocytes were collected 20 hours later by flushing with 10 ml of PBS. After red blood cell lysis, peritoneal cells were washed with staining buffer, and $3 \times 10^6$ cells were incubated with mouse anti-mouse CD16/CD32 (1:50; Caltag Laboratories) for 30 minutes to block Fc receptors. After washing, the peritoneal cells were incubated with antibodies for HSC/HPC markers, as described above, for 30 minutes. Cells were washed twice with staining buffer and analyzed by flow cytometry, as described above.

*APAP-induced liver injury*. WT and *Ccr2*$^{-/-}$ mice were fasted overnight before intraperitoneal challenge with 300 mg/kg of APAP (34). Fresh suspensions of APAP (Sigma-Aldrich) were made before each experiment by dissolving APAP powder in sterile PBS warmed to 45°C. PBS was used as a control.

*Competitive repopulation assays*. $CD45.2^+$ C57BL/6 WT and *Ccr2*$^{-/-}$ mice were treated with thioglycollate, as described above. After 24 hours, peritoneal leukocytes were collected by flushing with 10 ml of PBS. Lineage-negative cells were enriched by MACS using lineage cell depletion kit (AutoMACS; Miltenyi Biotec) according to the manufacturer's instructions and further purified by FACS sorting. Ten million WT $Lin^-$ (from 12 WT mice) or 6 million *Ccr2*$^{-/-}$ $Lin^-$ peritoneal leukocytes (from 12 *Ccr2*$^{-/-}$ mice) were injected into the tail veins of lethally irradiated (11 Gy) $CD45.1^+$ congenic mice. Unfractionated BM cells ($10^5$) from a common pool of $CD45.1^+$ donors were coinjected with peritoneal-derived $Lin^-$ WT or *Ccr2*$^{-/-}$ cells. At 8 and 16 weeks after the transplant, peripheral blood was obtained from a tail vein, and the presence of donor-derived myeloid cells ($CD45.2^+Gr\text{-}1^+$ and $CD45.2^+Mac\text{-}1^+$) or lymphoid cells ($CD45.2^+CD3^+$ and $CD45.2^+B220^+$) was assessed by flow cytometry. For secondary transplantation, $2 \times 10^6$ unfractionated BM mononuclear cells from primary recipients were isolated and transplanted into lethally irradiated (11 Gy) $CD45.1^+$ recipients. Sixteen weeks later, donor CD45.2 chimerism in peripheral blood was assessed by FACS analysis.

Primitive hematopoietic cells were isolated from the liver after APAP treatment. Lineage-negative and $CD45.2^+$ cells from the livers of CD45.2 mice were MACS enriched with CD11b magnetic beads (AutoMACS; Miltenyi Biotec) to deplete $CD11b^+$ cells and then FACS sorted. We collected $1 \times 10^6$ cells and mixed them with a common pool of CD45.1 unfractionated BM cells ($2 \times 10^5$) and coinjected the mixture into lethally irradiated CD45.1 recipients. Chimerisms were determined at 2 and 4 months after transplantation.

*Chimerism analysis by fluorescence cytometry*. Tail-vein blood samples (50 μl) were obtained 8 and 16 weeks after transplantation for analysis of donor chimerism and at 16 weeks for multilineage analysis of donor cells. Peripheral blood cells were incubated in red blood cell lysis buffer for 15 minutes at room temperature as described above. The cells were washed twice in PBS containing 0.1% BSA and resuspended for antibody staining for donor chimerism and multilineage analysis. Each sample was stained with CD45.1-FITC (B6.BoyJ strain) and CD45.2-APC (C57Bl/6 strain) or CD45.2 together with 5 individual lineage markers (CD3, Mac1, Grl, CD11c, and B220) conjugated to PE at 4°C for 20 minutes, washed twice, and analyzed by fluorescence cytometry. C57BL/6 and B6.BoyJ cells were stained with CD45.1 and CD45.2 individually as controls to determine the appropriate gate settings. A total of 10,000 events were collected from each sample.

*In vivo assessment of HSC/HPC proliferation and differentiation*. Twenty-four hours after thioglycollate treatment of CD45.1 WT mice, peritoneum-derived $Lin^-$ cells were sorted by FACS as described above and stained with CFSE at a final concentration of 2 mM (Molecular Probes; Invitrogen). The cell suspension was incubated at 37°C for 10 minutes and washed 3 times with cold PBS. Approximated $2 \times 10^6$ $Lin^-$ cells isolated from each CD45.1 WT mouse were injected into the peritoneum of a *Ccr2*$^{-/-}$ recipient mouse that had been challenged with thioglycollate. Two days after the implantation of the cells, mice were sacrificed, and leukocytes from the peritoneum were harvested. Cells were stained with a panel of monoclonal antibodies against myeloid and lymphoid lineage markers CD11b, CD11c, Gr-1, CD3, and B220, as described above.

*Adoptive BM transfer in APAP-treated mice*. $CD45.1^+$ WT mice were treated with APAP as described above. BM $Lin^-$ cells were FACS sorted from the BM of congenic $CD45.2^+$ WT or *Ccr2*$^{-/-}$ mice. After 3–5 hours, $CD45.1^+$ WT mice received $2 \times 10^6$ $Lin^-$ WT or *Ccr2*$^{-/-}$ cells by injection of the tail vein.

*Chemotaxis assay*. Chemotaxis studies were performed using 5-μm pore 24-well Boyden chamber (Neuro Probe). *gfp*$^{+/-}$ (*CX3CR1*) mice were used for the purpose of enriching the BM cells for early progenitors, as described (51).

$GFP^+c\text{-}Kit^+Lin^-$ BM cells were FACS sorted and washed twice with RPMI in 10% serum, and 3 to $6 \times 10^5$ cells were added to the upper chamber. Chemokines were used at the following concentrations: 20 ng/ml murine MCP-1 (R&D Systems), 500 ng/ml murine MCP-3, and 50 ng/ml SDF-1 (Peprotech) in 600 μl of RPMI in 10% serum in the lower chamber. Chambers were incubated for 4–10 hours at 37°C in a humidified incubator in the presence of 5% $CO_2$. Cells that migrated were quantified with the FACS LSRII, with appropriate gating on live cells. Input cells and migrated cells were stained with lineage markers (Gr1, CD3, B220, CD11b, Ter119), anti–c-Kit, anti–Sca-1, and anti-CD34 antibodies, as described above. To determine the migration capacity of clonogenic cells, 100 μl of the lower well content was plated for progenitor assays for the growth of CFUs, as described above.

*qRT-PCR*. RNA was isolated from FACS-sorted cell populations with the PicoPure RNA isolation kit (Molecular Devices) according to the manufacturer's instructions. Quantity was assessed with the Nanodrop 1000, and RNA was reverse-transcribed with TaqMan reverse transcription reagents. qRT-PCR was carried out with TaqMan PCR Master Mix, TaqMan gene expression assays, and an Applied Biosystems 7900HT thermal cycler. All TaqMan reagents were from Applied Biosystems. Reactions were run in triplicate, and the genes of interest were normalized to glyceraldehyde-3P-dehydrogenase.

*Statistics*. Data were analyzed with GraphPad Insert, version 3.0. A nonparametric Mann-Whitney *U* test and an unpaired 2-tailed Student's *t* test were used; $P < 0.05$ was considered significant. 1-way ANOVA was used for comparison of groups.

## Acknowledgments

We thank M. Mack for the generous gift of the anti-mCCR2 antibody, and D. Littman and S. Jung for the CX3CR1- GFP mice. We also thank Gary Howard and Stephen Ordway for editorial assistance, Daryl Jones for manuscript preparation, and John Carroll and Alisha Wilson for preparation of the figures. This work was funded in part by NIH grant R01 HL052773.

Received for publication June 25, 2009, and accepted in revised form January 20, 2010.

Address correspondence to: Israel F. Charo, Gladstone Institute of Cardiovascular Disease, 1650 Owens Street, San Francisco, CA 94158. Phone: 415.734.2000; Fax: 415.355.0960; E-mail: icharo@gladstone.ucsf.edu.

1. Goodman JW, Hodgson GS. Evidence for stem cells in the peripheral blood of mice. *Blood*. 1962;19:702–714.
2. Wright DE, Wagers AJ, Gulati AP, Johnson FL, Weissman IL. Physiological migration of hematopoietic stem and progenitor cells. *Science*. 2001;294(5548):1933–1936.
3. Massberg S, et al. Immunosurveillance by hematopoietic progenitor cells trafficking through blood, lymph, and peripheral tissues. *Cell*. 2007;131(5):994–1008.
4. Burt R, et al. Clinical applications of blood-derived and marrow-derived stem cells for nonmalignant diseases. *JAMA*. 2008;299(8):925–936.
5. Lee MS, Makkar RR. Stem-cell transplantation in myocardial infarction: a status report. *Ann Intern Med*. 2004;140(9):729–737.
6. Leone AM, et al. Mobilization of bone marrow-derived stem cells after myocardial infarction and left ventricular function. *Eur Heart J*. 2005;26(12):1196–1204.
7. Schachinger V, et al. Improved clinical outcome after intracoronary administration of bone-marrow-derived progenitor cells in acute myocardial infarction: final 1-year results of the REPAIR-AMI trial. *Eur Heart J*. 2006;27(23):2775–2783.
8. Gordon MY, et al. Characterization and clinical application of human CD34+ stem/progenitor cell populations mobilized into the blood by granulocyte colony-stimulating factor. *Stem Cells*. 2006;24(7):1822–1830.
9. Charo I, Myers S, Herman A, Fanci C, Connolly A, Coughlin S. Molecular cloning and functional expression of two monocyte chemoattractant protein 1 receptors reveals alternative splicing of the carboxyl-terminal tails. *Proc Natl Acad Sci U S A*. 1994;91(7):2752–2756.
10. Boring L, et al. Impaired monocyte migration and reduced type 1 (Th1) cytokine responses in C-C chemokine receptor 2 knockout mice. *J Clin Invest*. 1997;100(10):2552–2561.
11. Izikson L, Klein RS, Charo IF, Weiner HL, Luster AD. Resistance to experimental autoimmune encephalomyelitis in mice lacking the CC chemokine receptor (CCR)2. *J Exp Med*. 2000;192(7):1075–1080.
12. Peters W, Scott HM, Chambers HF, Flynn JL, Charo IF, Ernst JD. Chemokine receptor 2 serves an early and essential role in resistance to Mycobacterium tuberculosis. *Proc Natl Acad Sci U S A*. 2001;98(14):7958–7963.
13. Boring L, Gosling J, Cleary M, Charo IF. Decreased lesion formation in CCR2–/– mice reveals a role for chemokines in the initiation of atherosclerosis. *Nature*. 1998;394(6696):894–897.
14. Lu B, et al. Abnormalities in monocyte recruitment and cytokine expression in monocyte chemoattractant protein 1-deficient mice. *J Exp Med*. 1998;187(4):601–608.
15. Huang DR, Wang J, Kivisakk P, Rollins BJ, Ransohoff RM. Absence of monocyte chemoattractant protein 1 in mice leads to decreased local macrophage recruitment and antigen-specific T helper cell type 1 immune response in experimental autoimmune encephalomyelitis. *J Exp Med*. 2001;193(6):713–726.
16. Sozzani S, et al. Receptors and transduction pathways for monocyte chemotactic protein-2 and monocyte chemotactic protein-3. Similarities and differences with MCP-1. *J Immun*. 1994;152(7):3615–3622.
17. Serbina NV, Pamer EG. Monocyte emigration from bone marrow during bacterial infection requires signals mediated by chemokine receptor CCR2. *Nat Immunol*. 2006;7(3):311–317.
18. Tsou CL, et al. Critical roles for CCR2 and MCP-3 in monocyte mobilization from bone marrow and recruitment to inflammatory sites. *J Clin Invest*. 2007;117(4):902–909.
19. Kondo M, et al. Biology of hematopoietic stem cells and progenitors: implications for clinical application. *Annu Rev Immunol*. 2003;21:759–806.
20. Weissman IL, Shizuru JA. The origins of the identification and isolation of hematopoietic stem cells, and their capability to induce donor-specific transplantation tolerance and treat autoimmune diseases. *Blood*. 2008;112(9):3543–3553.
21. Reid S, et al. Enhanced myeloid progenitor cell cycling and apoptosis in mice lacking the chemokine receptor, CCR2. *Blood*. 1999;93(5):1524–1533.
22. Osawa M, et al. In vivo self-renewal of c-Kit+ Sca-1+ Lin(low/-) hemopoietic stem cells. *J Immunol*. 1996;156(9):3207–3214.
23. Bhattacharya D, Czechowicz A, Ooi AG, Rossi DJ, Bryder D, Weissman IL. Niche recycling through division-independent egress of hematopoietic stem cells. *J Exp Med*. 2009;206(12):2837–2850.
24. Mohle R, Bautz F, Rafii S, Moore M, Brugger W, Kanz L. The chemokine receptor CXCR-4 is expressed on CD34+ hematopoietic progenitors and leukemic cells and mediates transendothelial migration induced by stromal cell-derived factor-1. *Blood*. 1998;91(12):4523–4530.
25. Broxmeyer HE. Chemokines in hematopoiesis. *Curr Opin Hematol*. 2008;15(1):49–58.
26. Charo IF, Ransohoff RM. The many roles of chemokines and chemokine receptors in inflammation. *N Engl J Med*. 2006;354(6):610–621.
27. Tacke F, Randolph GJ. Migratory fate and differentiation of blood monocyte subsets. *Immunobiology*. 2006;211(6–8):609–618.
28. Nagai Y, et al. Toll-like receptors on hematopoietic progenitor cells stimulate innate immune system replenishment. *Immunity*. 2006;24(6):801–812.
29. Haug JS, et al. N-cadherin expression level distinguishes reserved versus primed states of hematopoietic stem cells. *Cell Stem Cell*. 2008;2(4):367–379.
30. Kuziel WA, et al. Severe reduction in leukocyte adhesion and monocyte extravasation in mice deficient in CC chemokine receptor 2. *Proc Natl Acad Sci U S A*. 1997;94(22):12053–12058.
31. Oelschlaegel U, et al. Kinetics of CXCR-4 and adhesion molecule expression during autologous stem cell mobilisation with G-CSF plus AMD3100 in patients with multiple myeloma. *Ann Hematol*. 2007;86(8):569–573.
32. Fowler CJ, et al. Rescue from failed growth factor and/or chemotherapy HSC mobilization with G-CSF and plerixafor (AMD3100): an institutional experience. *Bone Marrow Transplant*. 2009;43(12):909–917.
33. Serbina N, Pamer E. Monocyte emigration from bone marrow during bacterial infection requires signals mediated by chemokine receptor CCR2. *Nat Immunol*. 2006;7(3):311–317.
34. Hogaboam CM, et al. Exaggerated hepatic injury due to acetaminophen challenge in mice lacking C-C chemokine receptor 2. *Am J Pathol*. 2000;156(4):1245–1252.
35. Holt MP, Cheng L, Ju C. Identification and characterization of infiltrating macrophages in acetaminophen-induced liver injury. *J Leukoc Biol*. 2008;84(6):1410–1421.
36. Terai S, et al. Improved liver function in patients with liver cirrhosis after autologous bone marrow cell infusion therapy. *Stem Cells*. 2006;24(10):2292–2298.
37. Tendera M, Wojakowski W. Cell therapy--success does not come easy. *Eur Heart J*. 2009;30(6):640–641.
38. Charwat S, et al. Role of adult bone marrow stem cells in the repair of ischemic myocardium: current state of the art. *Exp Hematol*. 2008;36(6):672–680.
39. Reffelmann T, Konemann S, Kloner RA. Promise of blood- and bone marrow-derived stem cell transplantation for functional cardiac repair: putting it

in perspective with existing therapy. *J Am Coll Cardiol*. 2009;53(4):305–308.
40. Balsam LB, et al. Haematopoietic stem cells adopt mature haematopoietic fates in ischaemic myocardium. *Nature*. 2004;428(6983):668–673.
41. Wagers AJ, Weissman IL. Plasticity of adult stem cells. *Cell*. 2004;116(5):639–648.
42. Wagers AJ, Sherwood RI, Christensen JL, Weissman IL. Little evidence for developmental plasticity of adult hematopoietic stem cells. *Science*. 2002;297(5590):2256–2259.
43. Fazel S, et al. Cardioprotective c-kit+ cells are from the bone marrow and regulate the myocardial balance of angiogenic cytokines. *J Clin Invest*. 2006;116(7):1865–1877.
44. Di Campli C, et al. A human umbilical cord stem cell rescue therapy in a murine model of toxic liver injury. *Dig Liver Dis*. 2004;36(9):603–613.
45. Yannaki E, et al. G-CSF-primed hematopoietic stem cells or G-CSF per se accelerate recovery and improve survival after liver injury, predominantly by promoting endogenous repair programs. *Exp Hematol*. 2005;33(1):108–119.
46. Liu F, et al. Hematopoietic stem cells mobilized by granulocyte colony-stimulating factor partly contribute to liver graft regeneration after partial orthotopic liver transplantation. *Liver Transpl*. 2006;12(7):1129–1137.
47. Gu L, et al. Absence of monocyte chemoattractant protein-1 reduces atherosclerosis in low density lipoprotein receptor–deficient mice. *Mol Cell*. 1998;2(2):275–281.
48. Jung S, et al. Analysis of fractalkine receptor CX(3)CR1 function by targeted deletion and green fluorescent protein reporter gene insertion. *Mol Cell Biol*. 2000;20(11):4106–4114.
49. Weisberg SP, et al. Obesity is associated with macrophage accumulation in adipose tissue. *J Clin Invest*. 2003;112(12):1796–1808.
50. Mack M, et al. Expression and characterization of the chemokine receptors CCR2 and CCR5 in mice. *J Immunol*. 2001;166(7):4697–4704.
51. Fogg D, et al. A clonogenic bone marrow progenitor specific for macrophages and dendritic cells. *Science*. 2005;311(5757):83–87.